

Chaperone Proteins Select and Maintain $[PIN^+]$ Prion Conformations in *Saccharomyces cerevisiae*⁵

Received for publication, May 1, 2012, and in revised form, November 8, 2012. Published, JBC Papers in Press, November 12, 2012, DOI 10.1074/jbc.M112.377564

David L. Lancaster¹, C. Melissa Dobson, and Richard A. Rachubinski²

From the Department of Cell Biology, University of Alberta, Edmonton, Alberta T6G 2H7, Canada

Background: Prion proteins adopt different conformations, known as variants, each with a distinct phenotype.

Results: Deletion of specific chaperone genes (*HSC82*, *AHA1*, *CPR6*, *CPR7*, *SBA1*, *TAH1*, *SSE1*) alters established $[PIN^+]$ variants in *S. cerevisiae*.

Conclusion: Chaperone proteins have a role in determining prion variants.

Significance: Chaperone activity helps to regulate cell prion phenotype.

Prions are proteins that can adopt different infectious conformations known as “strains” or “variants,” each with a distinct, epigenetically inheritable phenotype. Mechanisms by which prion variants are determined remain unclear. Here we use the *Saccharomyces cerevisiae* prion Rnq1p/ $[PIN^+]$ as a model to investigate the effects of chaperone proteins upon prion variant determination. We show that deletion of specific chaperone genes alters $[PIN^+]$ variant phenotypes, including $[PSI^+]$ induction efficiency, Rnq1p aggregate morphology/size and variant dominance. Mating assays demonstrate that gene deletion-induced phenotypic changes are stably inherited in a non-Mendelian manner even after restoration of the deleted gene, confirming that they are due to a *bona fide* change in the $[PIN^+]$ variant. Together, our results demonstrate a role for chaperones in regulating the prion variant complement of a cell.

The mammalian prion protein, PrP, was originally identified as the causative agent of a group of neurodegenerative disorders collectively known as the transmissible spongiform encephalopathies (1). When the prion-determining domain (PrD) of PrP misfolds, PrP can switch from a non-infectious conformation (PrP^C) to a conformation prone to forming self-propagating, β -sheet-rich, amyloid polymers (PrP^{Sc}) (1, 2). These amyloids spread by catalyzing the transformation of PrP^C into PrP^{Sc}, eventually forming large aggregates (for review, see Ref. 3).

Although genetic polymorphisms of the PrP gene do affect its disease pathology (4, 5), distinct sets of symptoms arising from genetically identical PrP^{Sc}, called strains, have been described (6, 7). Protease treatment of different strains of PrP^{Sc} aggregates revealed that they differed by the size and composition of their amyloid core region, suggesting that it is specific conformations of the amyloid that give rise to PrP^{Sc} strains (8).

Prions have also been characterized in non-mammalian model organisms, including bakers' yeast, *Saccharomyces cerevisiae*, where they have been demonstrated to occur frequently in the wild (9–13). Yeast prions can also form different strains, called variants (14–16). Studies have shown that different prion conformations distinguish each prion variant (17–19).

The prion protein Rnq1p can adopt different variants, each with a distinct phenotype. Although the function of its non-prion conformation remains unknown, the prion conformation of Rnq1p, $[PIN^+]$, acts to help another yeast prion, Sup35p/ $[PSI^+]$, adopt its own prion state (20, 21). Rnq1p has a prion-determining domain between amino acids 153 and 405, with a non-prion domain N terminus (11). Some $[PIN^+]$ variants include $[PIN^+]^{\text{low}}$, $[PIN^+]^{\text{medium}}$, and $[PIN^+]^{\text{high}}$, each named for its respective $[PSI^+]$ induction efficiency (16). Another $[PIN^+]$ variant-linked phenotype is observed when GFP-tagged Rnq1p is overproduced *in vivo* (22). $[PIN^+]^{\text{high}}$ strains form multiple Rnq1-GFP foci per cell, whereas $[PIN^+]^{\text{medium}}$ and $[PIN^+]^{\text{low}}$ strains generally form only a single Rnq1-GFP focus. Another phenotypic difference between $[PIN^+]$ variants is the size and stability of their amyloid aggregates. $[PIN^+]^{\text{high}}$ contains less stable aggregates that break down into smaller sub-particles when heated, as opposed to $[PIN^+]^{\text{low}}$ or $[PIN^+]^{\text{medium}}$ aggregates, which remain stable when heated (16, 23, 24). When two $[PIN^+]$ variants are introduced into the same cell, either through mating or cytoduction, the diploid and all haploid progeny adopt the phenotype of the dominant variant. $[PIN^+]^{\text{high}}$ is dominant over $[PIN^+]^{\text{medium}}$, which is in turn dominant over $[PIN^+]^{\text{low}}$ (16). These multiple, distinct phenotypes make $[PIN^+]$ an ideal model system with which to study the etiology of prion variants.

Mutations in a prion protein can affect its amyloid structure and, through that, the type of variant it adopts (25, 26). Still, variants can arise from prion proteins with identical sequences (14–16, 27), suggesting that other cellular factors may influence the variant conformation that a given prion will adopt. Chaperone proteins are strong candidates for such variant regulating factors. Chaperones are known to affect the conformation of a wide array of client proteins (for review, see Ref. 28) and have been implicated in other aspects of prion biology, including the *de novo* formation, propagation, and curing of

⁵ This article contains supplemental Table S1 and Figs. S1–S5.

¹ Recipient of a Frederick Banting and Charles Best Canada Graduate Scholarship Doctoral Award from the Canadian Institutes of Health Research. To whom correspondence should be addressed: Dept. of Cell Biology, University of Alberta, Medical Sciences Building 5-14, Edmonton, Alberta T6G 2H7, Canada. Tel.: 780-492-7407; Fax: 780-492-0450; E-mail: dll1@ualberta.ca.

² An International Research Scholar of the Howard Hughes Medical Institute.

prions (for review, see Ref. 29–31). Additionally, changes to chaperone activity and levels have been shown to affect prion variants. Yeast strains expressing N- and C-terminal truncations of the primary stress response transcriptional regulator, Hsf1p, which were shown to increase Hsp104p and decrease Hsp90 levels, respectively, preferentially formed specific $[PSI^+]$ variants upon *de novo* induction (32). Likewise, strains over- or underexpressing *SSE1*, which is important to Hsp70 activity, gave rise to specific $[PSI^+]$ variants when induced (33). To date, only one genetic mutation has been reported to lead to a change in a pre-existing variant. Sondheimer *et al.* (27) demonstrated that deletion of the Sis1p G/F domain altered Rnq1-GFP aggregation pattern in a manner stably propagated even after reintroduction of wild-type Sis1p.

Here, we report the findings of our investigations into the actions of chaperone proteins upon already established $[PIN^+]$ variants. We found that disruption of several chaperone genes gives rise to shifts in $[PIN^+]$ variant-linked phenotypes. Genetic analysis showed that the phenotypic shifts are inherited in a non-Mendelian manner, confirming that a *bona fide* change in $[PIN^+]$ variant was achieved. Our findings provide evidence that chaperones can affect established prion variants and highlight a potential role for chaperones in regulating prion-linked phenotypes through their modulation of prion variants.

EXPERIMENTAL PROCEDURES

Yeast Strains, Culture, and Genetic Manipulation—*S. cerevisiae* strains used in this study are listed in supplemental Table S1. All yeast strains were cultured at 30 °C with the exception of diploids undergoing sporulation, which were cultured at 25 °C. Media were as follows: YEPD (1% yeast extract, 2% peptone, 2% glucose); CSM (0.67% yeast nitrogen base without amino acids, 2% glucose, 1 × Complete supplement mixture (Bio 101, Vista, CA)); CSM auxotrophic marker growth medium (same as CSM but containing 1 × CSM minus the appropriate auxotrophic selection (–ADE, –HIS, –LEU, –URA, –LYS-URA, –TRP-URA)); CSM auxotrophic marker induction medium (same as CSM but with 2% galactose in place of 2% glucose). For solid media, the same recipes were used with 2% agar added. Deletions were made using a *HIS3* cassette as described (34) and confirmed by PCR. Isogenic *MAT α* strains were made using YCpGAL::HO and mating-type switching (35). Mating, diploid sporulation, and dissection of haploids were performed as previously described with modified sporulation medium (0.3% potassium acetate, 0.02% raffinose) (36). Haploid progeny of dissections were tested for the presence of a gene deletion by culture on CSM-HIS plates.

Yeast Plasmids and Cloning—Plasmids used in this study were constructed as follows; pYES2.0-SUP35NM-GFP was constructed by ligating the sequence encoding enhanced GFP (37) in-frame with the 3'-end of base pairs 1–762 of the *SUP35* gene into pYES2.0 (Invitrogen). pYES2.0-GFP was similarly constructed with only the GFP-encoding sequence. pYES2.0-Rnq1-GFP was constructed by amplifying sequence coding for Rnq1p C-terminally tagged with GFP from genomic DNA of a commercially available GFP-tagged library strain (Invitrogen) and ligating it into pYES2.0. pGREG535-Rnq1 was constructed by amplifying *RNQ1* and inserting it into pGREG535 according

to the Drag & Drop protocol (38). Plasmids were verified by sequencing. *Escherichia coli* and yeast were transformed with plasmid using standard chemical transformation protocols (34, 39).

Assay for Nonsense Suppression—To quantify $[PSI^+]$ induction efficiency based upon nonsense suppression, Sup35NM-GFP or GFP alone was overproduced by culturing strains harboring pYES2.0-SUP35NM-GFP or pYES2.0-GFP, respectively, in liquid CSM medium for 24 h followed by subculturing in liquid CSM induction medium for 48 h. When testing primary deletions and diploids, cell cultures were normalized to an A_{600} of 1.0, and when testing tetrads, cultures were normalized to an A_{600} of 0.25. After normalization, 10-fold serial dilutions were made. 5 μ l of each dilution were spotted onto both CSM and CSM–ADE plates, and colony-forming units (cfu) were counted after 2 and 4 days, respectively. Percent $[PSI^+]$ induction efficiency was calculated as cfu (CSM–ADE)/cfu (CSM) × 100. Four to six independent experiments were performed for each strain.

Assay for Plasmid Retention—To determine if a given strain retained pYES2.0-SUP35NM-GFP, induced strains were plated for single colonies on both CSM and CSM–ADE, and colonies from both platings were then replica-plated onto CSM and CSM-URA media. Percent plasmid retention was calculated as cfu (CSM-URA)/cfu (CSM) × 100. Between 100 and 200 colonies were compared for each strain.

Assay for Prion Curing—To test induced $[PSI^+]$ strains for curability, colonies growing on CSM–ADE medium plates were streaked onto curing plates (YEPD + 3 mM guanidine HCl) and allowed to grow at 30 °C for 3 days. Putatively “cured” colonies were then selected based on their pigmentation, restreaked onto CSM and CSM–ADE plates, and allowed to grow at 30 °C for 2 and 4 days, respectively. At least four colonies were tested for each strain.

Characterization of Rnq1-GFP Aggregates in Vivo—Strains carrying pYES2.0-Rnq1-GFP were cultured for 24 h in liquid CSM growth medium then subcultured in liquid CSM induction medium for 24 h. The number of Rnq1-GFP foci per cell was then quantified by acquiring random wide-field micrographs of cells using an Olympus IX-80 fluorescence microscope. The frequency of multiple foci was expressed as a percentage of all cells containing multiple Rnq1-GFP foci. 800–1000 cells were counted and categorized over the course of 4 independent experiments.

Protein Analysis—Strains carrying pGREG535-Rnq1 were cultured for 24 h in liquid CSM growth medium, then subcultured in liquid CSM induction medium for 8 h. Protein samples were prepared and pelleted as described (24). The pellet fraction, enriched for insoluble HA-Rnq1p, was heated briefly at 55 °C and analyzed by semi-denaturing detergent-agarose gel electrophoresis (SDD-AGE)³ (24, 40). Blots were probed with anti-HA antibody (F-7 Sc7392, Santa Cruz Biotechnology, Santa Cruz, CA) and detected with HRP-conjugated anti-mouse IgG (GE Healthcare).

³ The abbreviation used is: SDD-AGE, semi-denaturing detergent-agarose gel electrophoresis.

Chaperone-mediated Determination of $[PIN^+]$ Variants

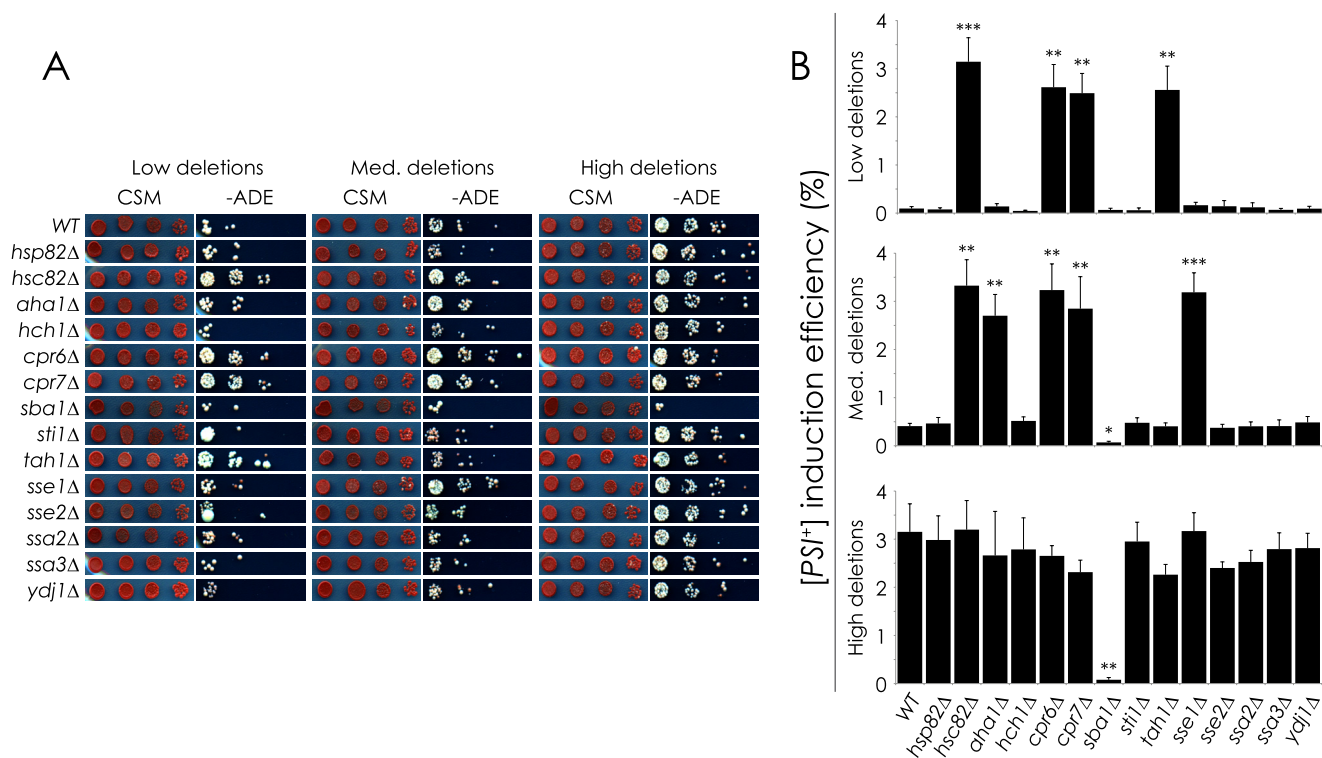


FIGURE 1. Effect of chaperone gene deletion on $[PSI^+]$ induction efficiency in relation to $[PIN^+]$ variants. A, shown is a nonsense suppression assay. Chaperone gene deletions were made in $[psi^-]$ $[PIN^+]^{low/med/high}$ strains that were induced to become $[PSI^+]$ by overproduction of Sup35NM-GFP. Normal growth is shown on CSM medium, and $[PSI^+]$ -dependent growth is shown on $-ADE$ medium. B, $[PSI^+]$ induction efficiency is shown. The efficiency of $[PSI^+]$ induction was determined by quantification of the nonsense suppression assay, expressing average $-ADE$ cfu as a percentage of average CSM cfu. Error bars represent S.E. Student's *t* tests were done to compare the $[PSI^+]$ induction efficiency of deletion strains with that of their parental wild-type strain. *, $p < 0.05$; **, $p < 0.01$; ***, $p < 0.001$.

Yeast Two-hybrid Analysis—Yeast two-hybrid analysis was performed using the yeast strain HF7c and the plasmids pGAD424 (prey) and pGBT9 (bait) (Clontech, Mountain View, CA) following standard protocols (41). Genes encoding Rnq1p or chaperone proteins were ligated in-frame into pGAD424 and pGBT9 for expression. Interactions were scored by growth of cells on CSM-HIS medium after 4 days of incubation relative to growth on YEPD. At least three independent experiments were done for each tested pair of proteins.

RESULTS

Deletion of Chaperone Genes Affects $[PSI^+]$ Induction Efficiency in a $[PIN^+]$ Variant-dependent Manner—To investigate the role of chaperones in $[PIN^+]$ variant determination, we made deletions of several chaperone-encoding genes in strains carrying characterized $[PIN^+]$ variants and measured changes in $[PSI^+]$ induction efficiency. Each strain was $[psi^-]$ and carried a nonsense-suppression reporter gene (*ADE1-14 UGA*) that allowed growth on CSM-*ADE* medium only when $[PSI^+]$ was induced (Fig. 1A). We measured the relative $[PSI^+]$ induction efficiencies of deletion strains using a nonsense suppression assay (Fig. 1B) as described under “Experimental Procedures.” In brief, we overproduced Sup35NM-GFP using the galactose-driven expression vector pYES2.0-SUP35NM-GFP and quantified cfu on CSM-*ADE* medium plates relative to cfu on CSM medium plates. The strength of the induced $[PSI^+]$ variants was not factored into our calculations of $[PSI^+]$ induction efficiency; only the number of colonies and not their size or pigmentation was considered.

Deletion of *HSC82*, *CPR6*, *CPR7*, or *TAH1* in the $[PIN^+]^{low}$ strain as well as *HSC82*, *AHA1*, *CPR6*, *CPR7*, or *SSE1* in the $[PIN^+]^{medium}$ strain increased strain growth on CSM-*ADE* medium to levels significantly higher than those of wild-type $[PIN^+]^{low}$ and wild-type $[PIN^+]^{medium}$ strains and similar to those of the wild-type $[PIN^+]^{high}$ strain. Deletion of these same genes in the $[PIN^+]^{high}$ strain did not affect $[PSI^+]$ induction efficiency. Conversely, deletion of *SBA1* in the $[PIN^+]^{medium}$ and $[PIN^+]^{high}$ backgrounds decreased the efficiency of $[PSI^+]$ induction to levels matching those of the wild-type $[PIN^+]^{low}$ strain but did not significantly decrease the efficiency of $[PSI^+]$ induction when deleted in the $[PIN^+]^{low}$ strain. Nearly all strains gave rise to colonies with variable levels of pigment ranging from pink to almost white (Fig. 1A). The only exception was the $[PIN^+]^{low}$ strain deleted for *TAH1* in which colonies were almost entirely white after induction, suggesting that the induced $[PSI^+]$ colonies all carry a strong $[PSI^+]$ variant.

ADE-competent colonies were confirmed to be prion-linked because they lost *ADE* competence after treatment with guanidine HCl (supplemental Fig. S1). Also, the extent of $[PSI^+]$ induction in a strain being dependent on the levels of plasmid retention by that strain was excluded as a possibility, as both wild-type and deletion strains retained plasmid at levels between 90 and 95% whether or not the cells were *ADE*-competent (data not shown).

Deletion of Chaperone Genes Affects the Aggregation of Rnq1p in a $[PIN^+]$ Variant-dependent Manner—Our results showing that the effects of gene deletion were $[PIN^+]$ variant-specific

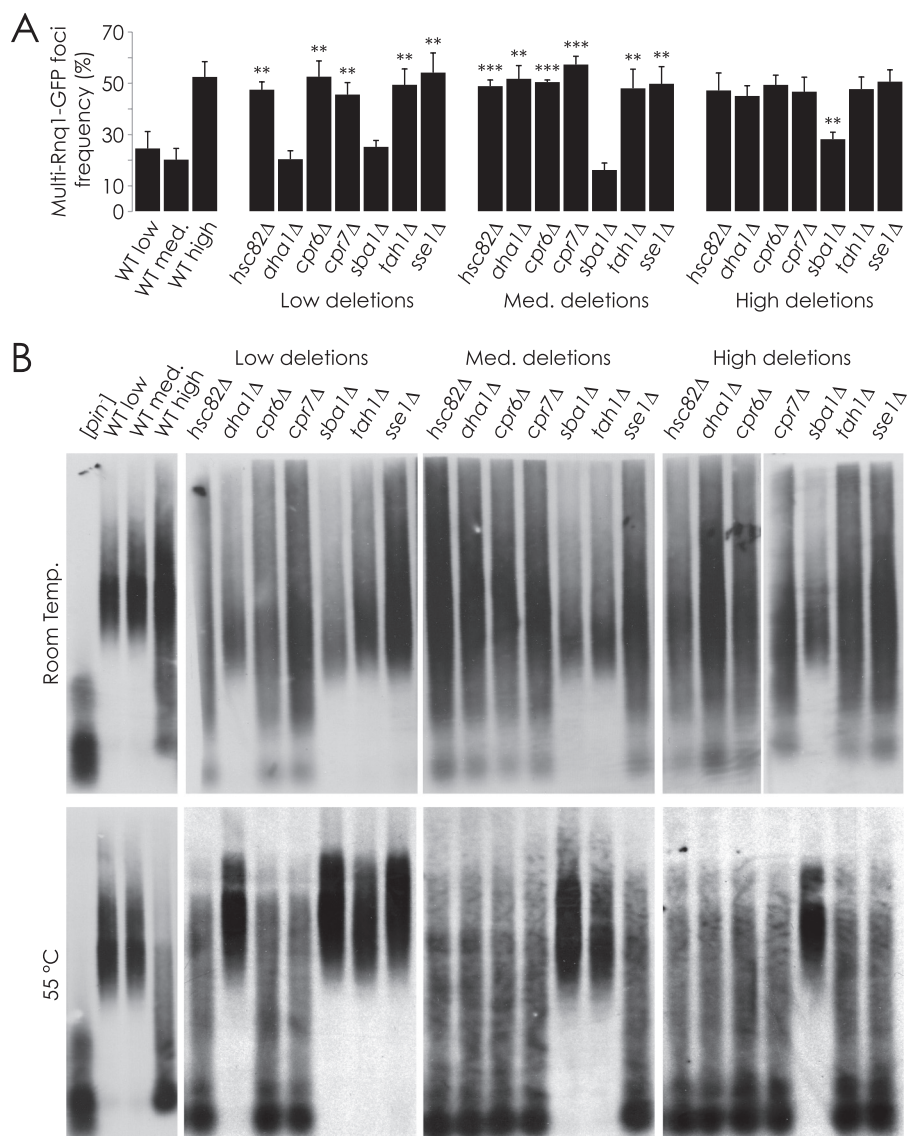


FIGURE 2. **Effect of chaperone gene deletion on $[PIN^+]$ variant-dependent phenotypes.** *A*, Rnq1-GFP was overproduced in deletion strains of interest, and the frequency of multiple Rnq1-GFP foci in foci-containing cells was calculated as a percentage of total cells. *Error bars* represent S.E. Student's *t* tests were performed to compare the frequency of multiple Rnq1-GFP foci in cells containing foci with that of their parental wild-type strain. **, $p < 0.01$; ***, $p < 0.001$. *B*, the Rnq1p aggregate size in deletion strains of interest was compared by SDD-AGE. Samples were incubated at room temperature (*top*) or 55 °C (*bottom*) before loading.

and resulted in shifts in $[PSI^+]$ induction efficiency from levels found in one wild-type variant strain, e.g. $[PIN^+]^{low}$, to a different wild-type variant strain, e.g. $[PIN^+]^{high}$, suggested that the chaperone gene deletions may have given rise to a change in the $[PIN^+]$ variant carried by the cell. If the $[PIN^+]$ variant of a strain had been altered by deletion of a chaperone gene, then other variant-specific phenotypes should also have been affected. Accordingly, we characterized the effects of chaperone gene deletion upon the phenotype of Rnq1p aggregates.

We first quantified the localization of Rnq1-GFP in all the deletion strains affected in $[PSI^+]$ induction efficiency (Fig. 2*A*). When GFP-tagged Rnq1p was overproduced from the galactose-driven plasmid pYES2.0-Rnq1-GFP, ~75% of focus-containing wild-type $[PIN^+]^{low}$ and wild-type $[PIN^+]^{medium}$ cells contained a single Rnq1-GFP focus, whereas ~25% contained more than one focus. ~50% of wild-type $[PIN^+]^{high}$ focus-containing cells contained multiple foci, in agreement with previ-

ous findings (22). $[PIN^+]^{low}$ and $[PIN^+]^{medium}$ strains deleted for the genes *HSC82*, *CPR6*, *CPR7*, *TAH1*, or *SSE1* that gave rise to increased $[PSI^+]$ induction also displayed multiple Rnq1-GFP foci at the frequency displayed by the wild-type $[PIN^+]^{high}$ strain. Deletion of *AHA1* in the $[PIN^+]^{medium}$ strain but not in the $[PIN^+]^{low}$ strain led to increased $[PSI^+]$ induction (Fig. 1*B*). Likewise, deletion of *AHA1* in the $[PIN^+]^{medium}$ strain but not in the $[PIN^+]^{low}$ strain led to an increase in multiple Rnq1-GFP foci to the frequency exhibited by the wild-type $[PIN^+]^{high}$ strain. In contrast, deletion of the *SBA1* gene from the $[PIN^+]^{high}$ strain led to fewer cells with multiple Rnq1-GFP foci, consistent with the frequencies exhibited by wild-type $[PIN^+]^{low}$ and wild-type $[PIN^+]^{medium}$ strains. Interestingly, increases in the number of multiple Rnq1-GFP foci were also observed when *TAH1* and *SSE1* were deleted in $[PIN^+]^{medium}$ and $[PIN^+]^{low}$ strains, respectively, even though there was no observed increase in $[PSI^+]$ induction efficiency in these deletion strains.

Chaperone-mediated Determination of $[PIN^+]$ Variants

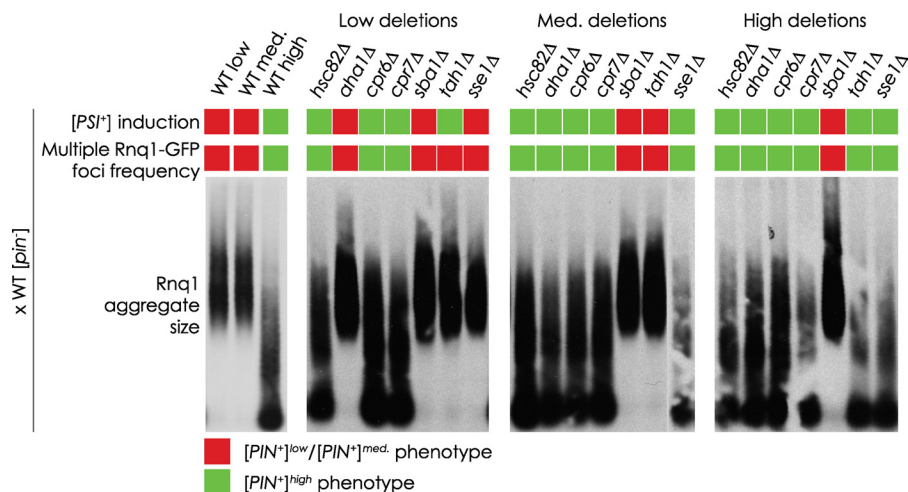


FIGURE 3. Maintenance of chaperone gene deletion-induced changes in $[PIN^+]$ variant-dependent phenotypes. Chaperone deletion strains were mated with a wild-type $[psi^-][pin^-]$ strain, and the resulting diploids were analyzed for $[PSI^+]$ induction efficiency, frequency of multiple Rnq1-GFP foci in cells containing foci, and Rnq1p aggregate size. These phenotypes were then categorized as either $[PIN^+]^{low/medium}$ or $[PIN^+]^{high}$. Quantifications of $[PSI^+]$ induction efficiency and frequency of multiple Rnq1-GFP foci in foci-containing cells can be found in [supplemental Fig. S2](#).

We next characterized the sizes of Rnq1p amyloid subparticles in the deletion strains. The sizes of Rnq1p amyloid subparticles have been shown to vary depending on whether the $[PIN^+]$ variant displays a single Rnq1-GFP focus per cell, as with the wild-type $[PIN^+]^{low}$ and wild-type $[PIN^+]^{medium}$ strains, or multiple foci per cell as observed in the wild-type $[PIN^+]^{high}$ strain (23). Strains with a single focus display a relatively narrow range of large subparticles, whereas strains with multiple foci display subparticles ranging in size from monomer to as large as, or larger than, those found in strains with a single focus. Accordingly, we produced HA-tagged Rnq1p from the plasmid pGREG535-Rnq1 in the wild-type $[PIN^+]^{low}$, $[PIN^+]^{medium}$, and $[PIN^+]^{high}$ strains and in these strains harboring a gene deletion. We then prepared samples enriched for proteins in an insoluble prion state and incubated them at room temperature and 55 °C, as Rnq1p aggregates purified from strains with multiple Rnq1p foci, specifically $[PIN^+]^{high}$, have been shown to be more sensitive to changes in temperature and to degrade partially at moderately elevated temperatures, whereas other Rnq1p variant aggregates do not (24). Finally, we compared the sizes of the purified HA-Rnq1p amyloid aggregates using SDD-AGE (Fig. 2B). We found that deleting *SBA1* in the wild-type $[PIN^+]^{high}$ strain eliminated small HA-Rnq1p amyloid aggregates, leaving a narrower range of larger aggregates, consistent with the patterns observed in the wild-type $[PIN^+]^{low}$ and wild-type $[PIN^+]^{medium}$ strains. Conversely, we observed that *hsc82Δ*, *aha1Δ*, *cpr6Δ*, *cpr7Δ*, and *sse1Δ* strains, which increased the efficiency of $[PSI^+]$ induction in $[PIN^+]^{low}$ and/or $[PIN^+]^{medium}$ backgrounds to levels observed in the wild-type $[PIN^+]^{high}$ strain, exhibited amyloid aggregates with a broader range of sizes, consistent with aggregates from the wild-type $[PIN^+]^{high}$ strain. These aggregates, like wild-type $[PIN^+]^{high}$ aggregates, also proved to be sensitive to temperature, degrading in part to a monomer at 55 °C (Fig. 2B). It is important to note that the pattern of protein migration displayed by these partly degraded protein aggregates is easily distinguished from that produced by protein aggregates isolated from a $[pin^-]$ strain. $[pin^-]$ aggregates were monomeric and of

low molecular weight, whereas partially degraded aggregates from $[PIN^+]$ strains still displayed species of high molecular weight. Our results suggest that deletion of specific chaperone genes leads to changes in the prion amyloid physical properties, thereby affecting its heat sensitivity.

Our results show a correlation between chaperone gene deletion strains displaying altered $[PSI^+]$ induction efficiency and those displaying changes in other $[PIN^+]$ -linked phenotypes. The *tah1Δ* strains were exceptions. They were unaffected in the sizes of their HA-Rnq1p aggregates *vis à vis* the sizes of the aggregates in their corresponding wild-type $[PIN^+]$ variant background. Also of note is that although the *sse1Δ* strain in the $[PIN^+]^{low}$ background showed multiple Rnq1-GFP foci per cell, its aggregates were limited to a narrow range of large sizes.

Deletion-induced Phenotypes Are Inherited in a Non-Mendelian Manner—The $[PIN^+]$ variant-linked phenotypic changes we observed in strains deleted for chaperone genes could be due directly to the effects of gene deletion or could be due simply to changes in the cell chaperone complement and to the overproduction of tagged protein resulting from our methodology. For example, loss of a chaperone could impair the ability of the cell to deal with the overexpression of tagged Rnq1p, leading to formation of denatured, non-prion aggregates that are detectable in our assays as multiple Rnq1-GFP foci and/or low molecular weight aggregates in SDD-AGE. To eliminate this trivial explanation and to confirm that it is indeed deletion of the chaperone genes that gives rise to the observed $[PIN^+]$ variant shifts, we reintroduced a wild-type copy of a deleted chaperone gene by crossing a deletion strain with an isogenic wild-type strain. This wild-type strain was $[pin^-]$ so as to avoid any convolution related to introducing dominant $[PIN^+]$ variants (16). If the effects of deletions were specific to the deletion of the gene, then restoring the chaperone gene would be expected to restore the original $[PIN^+]$ variant phenotype. If on the other hand a permanent change in the $[PIN^+]$ variant had occurred in the deletion strain, then the phenotypic changes should persist after reintroduction of the chaperone gene. Fig. 3 shows that, for the most part, $[PSI^+]$ induction efficiencies, the frequency of

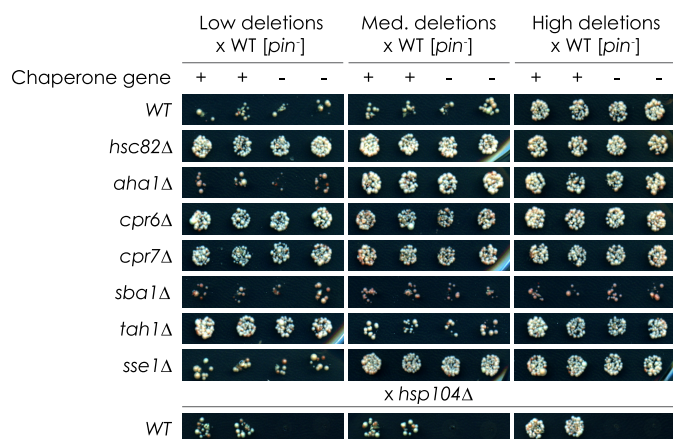


FIGURE 4. Non-Mendelian inheritance of chaperone gene deletion-induced changes in $[PSI^+]$ induction efficiency. Diploids generated by mating chaperone deletion strains with a wild-type $[psi^-][pin^-]$ strain were sporulated and dissected. The resulting tetrads were analyzed for $[PSI^+]$ induction efficiency by nonsense suppression assay on $-ADE$ medium. Wild-type strains were mated with $hsp104\Delta$ strains to demonstrate genetic specificity for this assay. Wild-type (+) and deletion-carrying (-) haploid progeny are presented. Twenty-four tetrads were analyzed per diploid.

Rnq1-GFP foci, and the sizes of Rnq1p aggregates of diploid strains did not revert to the phenotypes of the original wild-type strains from which the deletion strains were derived. Instead, these diploid strains maintained the phenotypes of the deletion strains. The only exceptions were diploids arising from matings with $sse1\Delta$ in the $[PIN^+]^{low}$ background and with $tah1\Delta$ in both the $[PIN^+]^{low}$ and $[PIN^+]^{medium}$ backgrounds. The increased frequency of Rnq1-GFP foci in the original haploid strains deleted for $SSE1$ or $TAH1$ was eliminated in the diploid strains, suggesting that these changes were $[PIN^+]$ -independent. It should be noted that under our experimental conditions we were unable to statistically distinguish $[PIN^+]^{low}$ from $[PIN^+]^{medium}$ based upon $[PSI^+]$ induction efficiencies (supplemental Fig. S2). As such, we could categorize our results only as being consistent with either $[PIN^+]^{low/medium}$ or $[PIN^+]^{high}$ levels.

There was the remote possibility that spurious mutations had been introduced into our deletion strains and had produced dominant effects mimicking an apparent variant switch. If this were the case, it would be expected that this trait would be co-inherited in a Mendelian manner as opposed to the non-Mendelian manner of a true change in variant. To eliminate the possibility of introduced spurious mutations, we sporulated and dissected our diploid strains, yielding wild-type and deletion-carrying haploid progeny. The presence of the chaperone gene deletion cassette ($HIS3$) was detected by growth on CSM-HIS medium and showed a 2:2 ratio in the progeny as expected (data not shown). We then measured $[PSI^+]$ induction efficiency of the dissected tetrads by nonsense suppression assay (Fig. 4). The specificity of this assay was demonstrated by mating wild-type strains carrying different $[PIN^+]$ variants with a strain deleted for $HSP104$, which is required for both $[PSI^+]$ and $[PIN^+]$ maintenance (20, 42). The wild-type haploid progeny were inducible at levels similar to their parental strains, whereas the $hsp104\Delta$ haploids were unable to be induced. When the chaperone gene deletion strains were mated with the wild-type $[pin^-]$ strain, we found that the haploid progeny of 24

tetrads all maintained the same $[PSI^+]$ induction efficiency as the parental deletion strain regardless of the presence or absence of the chaperone gene of interest. These levels were consistent with either $[PIN^+]^{low/medium}$ or $[PIN^+]^{high}$ levels. Haploid progeny were found to retain pYES2.0-Sup35NM-GFP at a rate consistent with the parental strains, with no strain losing or retaining the plasmid at a markedly higher level than any other strain. Also, putative $[PSI^+]$ colonies that arose after $[PSI^+]$ induction were shown to be curable by growth on medium containing guanidine HCl (supplemental Fig. S3).

The Rnq1p aggregates of wild-type and mutant haploid progeny derived from the mating of deletion strains that gave rise to $[PIN^+]$ variant-related phenotypic changes were characterized using SDD-AGE (Fig. 5). We found that the deletion-induced changes in aggregate size were stable even after tetrad dissection. Deletion strains that exhibited no change in aggregate size were found to be consistent with the wild-type strain in which they were made (data not shown). Taken altogether, our results show that deletion of chaperone genes gives rise to *bona fide* changes in $[PIN^+]$ variant.

The Hierarchy of Inheritance of Induced Variants Is Consistent with Characterized $[PIN^+]$ Variants—Another characteristic of prion variants is that one is often dominant over another. In the case of $[PIN^+]$ variants, $[PIN^+]^{high}$ is dominant over $[PIN^+]^{medium}$, which in turn is dominant over $[PIN^+]^{low}$ (16). In most cases, deletion-induced variants display phenotypes comparable with $[PIN^+]^{high}$, with the exception of $sba1\Delta$, which gives rise to a variant similar to $[PIN^+]^{low/medium}$. Still, it remained unclear if these variants were actually $[PIN^+]^{high}$, $[PIN^+]^{low/medium}$, or novel, previously uncharacterized types of variants. If these variants were not novel, then they would be expected to follow the same hierarchy of variant dominance in relation to other $[PIN^+]$ variants. To determine the hierarchy of the induced variants, we crossed deletion strains to isogenic wild-type strains carrying $[PIN^+]^{low}$, $[PIN^+]^{medium}$, or $[PIN^+]^{high}$. We then documented the $[PIN^+]$ variant-related phenotypes of the resulting diploid strains (Fig. 6). As before, we were unable to distinguish statistically $[PIN^+]^{low}$ from $[PIN^+]^{medium}$ based on their $[PSI^+]$ induction efficiencies (supplemental Fig. S4).

We found that diploids generated by mating putative $[PIN^+]^{high}$ strains with any wild-type strain exhibited phenotypes consistent with wild-type $[PIN^+]^{high}$. Also, the presumed $[PIN^+]^{low/medium}$ variant induced by the deletion of $SBA1$ was shown to be eliminated by the introduction of the more dominant $[PIN^+]^{high}$. In the case of $tah1\Delta$ generated in $[PIN^+]^{low}$, its $[PIN^+]^{high}$ -like $[PSI^+]$ induction efficiency was dominant over $[PIN^+]^{low/medium}$ wild-type phenotypes, whereas wild-type $[PIN^+]^{high}$ was dominant over its other $[PIN^+]$ -linked phenotypes. Finally, the frequency of $[PIN^+]^{high}$ -like Rnq1-GFP foci observed when $SSE1$ was deleted in a $[PIN^+]^{low}$ strain reverted to a $[PIN^+]^{low/med}$ -like phenotype when mated with a wild-type $[PIN^+]^{low}$ strain or a wild-type $[PIN^+]^{medium}$ strain. All other traits followed wild-type patterns of inheritance.

Rnq1p Interacts Physically with Chaperone Proteins—We performed a yeast two-hybrid analysis to investigate possible physical interactions between our chaperones of interest and Rnq1p (Fig. 7). With growth on CSM-HIS medium as a reporter

Chaperone-mediated Determination of $[PIN^+]$ Variants

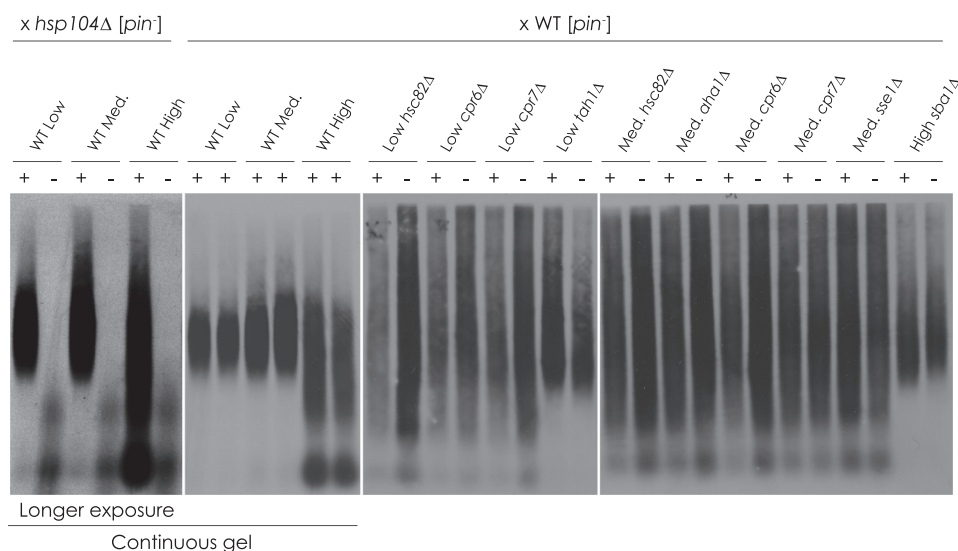


FIGURE 5. Non-Mendelian inheritance of chaperone gene deletion-induced changes in HA-Rnq1p aggregate size. Diploids generated by mating chaperone deletion strains with a wild-type $[psi^-][pin^-]$ strain were sporulated and dissected. The resulting tetrads were analyzed for HA-Rnq1p aggregate size by SDD-AGE. Wild-type strains were mated with $hsp104\Delta$ strains to demonstrate genetic specificity for this assay. Wild-type (+) and deletion-carrying (-) haploid progeny are presented. The $hsp104\Delta$ samples and wild-type controls were run on a continuous gel and exposed for a longer period. Twenty-four tetrads were analyzed per diploid.

of interaction, we detected a previously documented interaction between Rnq1p and Tah1p (43). We also identified two novel interactions: Cpr7p and Sba1p with Rnq1p. No interaction was detected between the remaining chaperones and Rnq1p. When we characterized the $[PIN^+]$ variant of our yeast two-hybrid strain (HF7c) by SDD-AGE and localization of Rnq1-GFP (supplemental Fig. S5), we found HF7c to be $[pin^-]$, suggesting that the interactions we detected occur when Rnq1p is in its non-prion conformation.

DISCUSSION

Although recombinant *S. cerevisiae* prion proteins do not require cofactors to misfold into multiple infectious variants *in vitro*, they need the activity of different chaperone proteins to propagate stably *in vivo*. Most prominent among these chaperones are Hsp104p, Sis1p, and members of the Ssa subfamily (for review, see Refs. 29–31). Together these chaperones facilitate the fragmentation of growing amyloid fibrils, thereby exposing more fibril growing ends and generating more infectious prion seeds. It has been proposed that conformational differences between variants alter their susceptibility to fragmentation and their rate of fibril growth and that equilibrium between these processes determines the stability of prion propagation and the strength of prion phenotype (18, 44, 45). For example, compared with $[PSI^+]^{weak}$, $[PSI^+]^{strong}$ has a smaller amyloid core that fragments more easily, allowing for the generation of more growing ends and a higher rate of Sup35p incorporation into a greater number of prion seeds (18). These seeds in turn lead to increased nonsense suppression and more stable propagation of $[PSI^+]$. Chaperones have also been implicated in variant determination, with alteration of Hsf1p or Sse1p activity affecting the *de novo* induction of the $[PSI^+]$ variant and truncation of Sis1p leading to stable changes in the established $[PIN^+]$ variant (27, 32, 33).

Our study provides further evidence that chaperones are important for the selection of prion variants. Deletion of *AHA1*

in a $[PIN^+]^{medium}$ background or deletion of *HSC82*, *CPR6*, or *CPR7* in either a $[PIN^+]^{low}$ or a $[PIN^+]^{medium}$ background increases the efficiency of $[PSI^+]$ induction to levels comparable to those seen for the wild-type $[PIN^+]^{high}$ strain. Conversely, deletion of *SBA1* in the $[PIN^+]^{high}$ background decreases the efficiency of $[PSI^+]$ induction to wild-type $[PIN^+]^{low/medium}$ levels.

Could the effects of deleting these chaperone-encoding genes on $[PSI^+]$ induction be independent of $[PIN^+]$? For example, the $[PIN^+]$ variant-specific effects on $[PSI^+]$ induction could be explained by different chaperone requirements for the *de novo* formation of $[PSI^+]$ in the presence of different $[PIN^+]$ variants. This scenario is not without precedent, as a $[PSI^+]$ variant with exceptionally large aggregates was shown to require increased Hsp104p levels to propagate stably (46). However, such a scenario is unlikely in our case, because the changes we observed in $[PSI^+]$ induction in our chaperone gene deletion strains were also accompanied by changes in the size and localization pattern of Rnq1p, consistent with a shift in $[PIN^+]$ variant. Additionally, these phenotypic shifts persist after sporulation of diploids into wild-type and deletion-carrying haploid progeny upon reintroduction of the deleted chaperone gene. Together, our results demonstrate that the chaperone gene deletion-induced phenotypes we observed are due to stable shifts in the $[PIN^+]$ variant.

Like other chaperone gene deletions, deletion of *TAH1* or *SSE1* in the $[PIN^+]^{low}$ or $[PIN^+]^{medium}$ backgrounds gave rise to changes in $[PIN^+]$ variant-dependent phenotypes. However, in contrast to what was observed for the other chaperone gene deletion strains, not all of the tested phenotypes were altered in *TAH1* or *SSE1* gene deletion strains, and of those phenotypes that were altered, not all were maintained after the wild-type gene was restored. This suggests that at least some of the changes observed in the *tah1Δ* and *sse1Δ* strains are not the result of shifts in the $[PIN^+]$ variant and that any putative var-

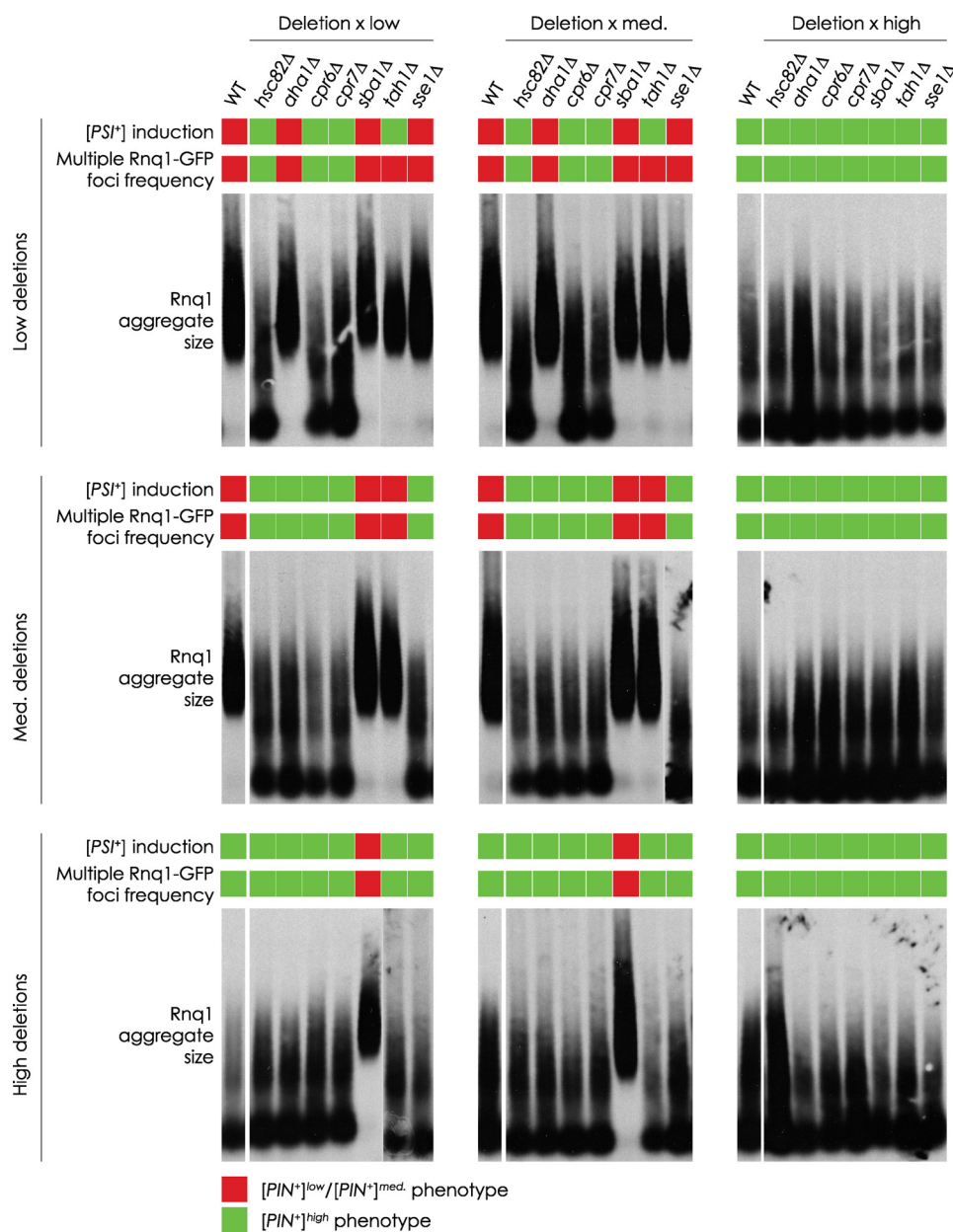


FIGURE 6. **Dominance of chaperone gene deletion-induced variants.** Diploids were generated by mating chaperone deletion stains with a wild-type $[psi^-]$ strain carrying the $[PIN^+]^{low}$ or $[PIN^+]^{medium}$ or $[PIN^+]^{high}$ variant. These diploids were analyzed for $[PSI^+]$ induction efficiency, frequency of multiple Rnq1-GFP foci in foci-containing cells, and Rnq1 p aggregate size. These phenotypes were then categorized as either $[PIN^+]^{low/medium}$ or $[PIN^+]^{high}$. Quantification of $[PSI^+]$ induction efficiency and frequency of multiple Rnq1-GFP foci in foci-containing cells can be found in supplemental Fig. S4.

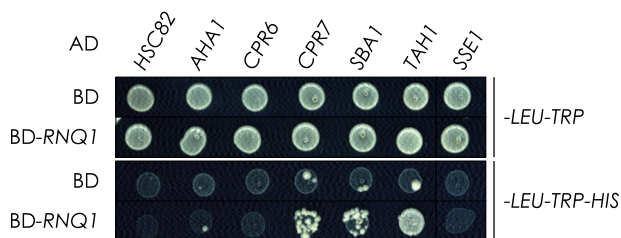


FIGURE 7. **Yeast two-hybrid analysis.** Cpr7p, Sba1p, and Tah1p were found to interact with Rnq1p based on growth of yeast on selective CSM-HIS medium. Total growth (top) and growth arising from protein interaction (bottom) are shown. The pattern presented is representative of four independent experiments. AD, activation domain; BD, binding domain.

variant shift that may have occurred in these deletion strains does not correspond to a previously characterized variant (16, 22). In contrast, variants arising from deletion of *HSC82*, *AHA1*, *CPR6*, or *CPR7* are consistent with $[PIN^+]^{high}$, whereas variants in *sba1Δ* strains match $[PIN^+]^{low}$ or $[PIN^+]^{medium}$. These deletion-induced variants may eventually be shown to be distinct from classical $[PIN^+]$ variants but for the purpose of discussion are referred to here as $[PIN^+]^{high}$ and $[PIN^+]^{low/medium}$, respectively.

$[PIN^+]^{high}$ phenotypes were readily identified, but $[PIN^+]^{low}$ and $[PIN^+]^{medium}$ were difficult to distinguish from each other. Their $[PSI^+]$ induction efficiencies did not vary greatly, and the properties of their aggregates were indistinguishable. As such, it is interesting that deletion of *AHA1*, *TAH1*, or *SSE1* had spe-

Chaperone-mediated Determination of $[PIN^+]$ Variants

cific effects depending upon whether they were deleted in $[PIN^+]^{low}$ or $[PIN^+]^{medium}$ backgrounds. This finding reinforces that $[PIN^+]^{low}$ and $[PIN^+]^{medium}$ are distinct variants and that these chaperone genes could serve as a genetic fingerprint for experimentally differentiating between the two variants in future studies.

By what mechanism might the variant changes we observed occur? Hsc82p, Aha1p, Cpr6p, Cpr7p, and Sba1p are known to act in the Hsp90 cycle (for review, see Ref. 47); Hsc82p is the constitutively expressed isomer of Hsp90; Aha1p, Cpr6p, and Cpr7p have been shown to increase Hsp90 ATP hydrolysis; Sba1p, the yeast homologue of p23, stabilizes the Hsp90-client complex, thereby decreasing Hsp90 ATPase activity (48–51). Our finding that deleting genes linked to increased Hsp90 ATPase activity led to a $[PIN^+]^{high}$ phenotype whereas deleting *SBA1* led to a $[PIN^+]^{low/medium}$ phenotype suggests that Hsp90 activity is important for variant determination, with Rnq1p a possible Hsp90 client. This possibility is supported by the finding that a strain expressing a C-terminal truncation of Hsf1p and predisposed to form unstable $[PSI^+]$ also had markedly decreased Hsp90 levels (32).

We detected physical interactions of Rnq1p with Cpr7p, Sba1p, and Tah1p but not with the other chaperones. This suggests that some of these chaperones may act upon Rnq1p independently of Hsp90. Cpr7p, for example, has intrinsic proline isomerase activity (52, 53). Rnq1p contains three proline residues: one in the N-terminal region, a region shown to affect prion propagation (54), and two in a putative loop region between the β -sheets of the amyloid core (55). Isomerization of these prolines could potentially affect Rnq1p conformation.

Additionally, as numerous physical interactions between these chaperones and other chaperone complexes have been documented, changes in the levels of these chaperones may affect how Hsp40s, Hsp70s, and/or Hsp104p interact with Rnq1p, resulting in variant change. Cpr7p, for example, has been shown to interact with Hsp104p in a manner that is not essential for its thermotolerance activity (56, 57). Additionally, inhibition of Hsp90 ATPase activity has been shown to increase the levels of both Hsp104p and Hsp70 (58). The effect of *SSE1* deletion that we report here also implicates Hsp70s in variant change, as *SSE1* encodes an important Hsp70 nucleotide exchange factor (59). Fan *et al.* found that manipulation of *Sse1p* levels affected the $[PSI^+]$ variant (33), although our *sse1 Δ* strain did not display the same disposition toward an unstable weak $[PSI^+]$ variant. The difference between our and their results could be due to $[PIN^+]$ variant-specific effects, as Fan *et al.* (33) did not characterize the $[PIN^+]$ variant of their strain. It is also interesting that it has been reported that mutations in *Sis1p* give rise to an increase in Rnq1-GFP foci (27), similar to what we observed. It may be that our gene deletions indirectly impaired the activity of *Sis1p* and/or its association with Rnq1p.

How the loss of specific chaperones alters the levels and activities of other chaperones, in addition to their interaction with Rnq1p, will be an important avenue of future investigation to clarify the mechanisms underlying the variant changes that we observed. Chaperones could mediate $[PIN^+]$ variant changes by altering the conformation of Rnq1p. For example, chaperones could regulate the folding of monomeric Rnq1p in

such a way as to predispose it to adopt a specific variant upon *de novo* formation or upon encountering prion seeds. More likely, because we observed changes to established variants, chaperones could work together to affect the conformation of existing amyloid polymers. For this to be effective, only the growing ends of polymers need be remodeled. Alternatively, if multiple or unstable variants are present at the same time in the cell, as has been shown to occur for $[PSI^+]$ (60), changes in the chaperone environment could alter the rates of amyloid polymer fragmentation and/or prion seed generation in a variant-specific manner. In this way, one variant could be selected over others.

In closing, we have demonstrated that altering the chaperone complement of a cell can alter existing prion variants without the introduction of exogenous prion material. By modulating existing prion variants, the cell can maintain prion seeds within the cell while mitigating potential negative effects of stronger prion phenotypes. Also, when environmental pressures demand, the existing prion variant could be quickly altered to provide a more advantageous phenotype to the cell. In light of recent findings reporting the prevalence of prions in wild strains of yeast as well as the apparent survival advantages that they bestow (13), prion variant regulation represents a powerful mechanism for modulating a cell response and adaptability to changing environmental conditions.

Acknowledgments—We thank Susan Liebman (University of Illinois) for wild-type $[PIN^+]$ variant strains and Troy Locke (Microarray and Proteomics Facility, University of Alberta) for help in screening haploid progeny of genetic crosses. We also thank Richard Poirier, Hanna Krolczak, Dwayne Weber, and Elena Savidov for technical assistance and Christopher Power, Paul Melançon, Paul LaPointe, Andrei Fagarasanu, Barbara Knoblach, Jinlan Chang, Robert Tower, Fred Mast, and Erin Brown for helpful discussion.

REFERENCES

1. Prusiner, S. (1982) Novel proteinaceous infectious particles cause scrapie. *Science* **216**, 136–144
2. Pan, K. M., Baldwin, M., Nguyen, J., Gasset, M., Serban, A., Groth, D., Mehlhorn, I., Huang, Z., Fletterick, R. J., and Cohen, F. E. (1993) Conversion of α -helices into β -sheets features in the formation of the scrapie prion proteins. *Proc. Natl. Acad. Sci. U.S.A.* **90**, 10962–10966
3. Colby, D. W., and Prusiner, S. B. (2011) Prions. *Cold Spring Harb. Perspect. Biol.* **3**, a006833
4. Brown, K., and Mastrianni, J. A. (2010) The prion diseases. *J. Geriatr. Psychiatry Neurol.* **23**, 277–298
5. Ohhashi, Y., Ito, K., Toyama, B. H., Weissman, J. S., and Tanaka, M. (2010) Differences in prion strain conformations result from non-native interactions in a nucleus. *Nat. Chem. Biol.* **6**, 225–230
6. Fraser, H., and Dickinson, A. G. (1968) The sequential development of the brain lesion of scrapie in three strains of mice. *J. Comp. Pathol.* **78**, 301–311
7. Bruce, M. E. (1993) Scrapie strain variation and mutation. *Br. Med. Bull.* **49**, 822–838
8. Bessen, R. A., and Marsh, R. F. (1994) Distinct PrP properties suggest the molecular basis of strain variation in transmissible mink encephalopathy. *J. Virol.* **68**, 7859–7868
9. Wickner, R. B. (1994) [URE3] as an altered URE2 protein. Evidence for a prion analog in *Saccharomyces cerevisiae*. *Science* **264**, 566–569
10. Paushkin, S. V., Kushnirov, V. V., Smirnov, V. N., and Ter-Avanesyan, M. D. (1996) Propagation of the yeast prion-like $[\psi^+]$ determinant is

- mediated by oligomerization of the *SLIP35*-encoded polypeptide chain release factor. *EMBO J.* **15**, 3127–3134
11. Sondheimer, N., and Lindquist, S. (2000) Rnq1. An epigenetic modifier of protein function in yeast. *Mol. Cell* **5**, 163–172
 12. Alberti, S., Halfmann, R., King, O., Kapila, A., and Lindquist, S. (2009) A systematic survey identifies prions and illuminates sequence features of prionogenic proteins. *Cell* **137**, 146–158
 13. Halfmann, R., Jarosz, D. F., Jones, S. K., Chang, A., Lancaster, A. K., and Lindquist, S. (2012) Prions are a common mechanism for phenotypic inheritance in wild yeasts. *Nature* **482**, 363–368
 14. Derkatch, I. L., Chernoff, Y. O., Kushnirov, V. V., Inge-Vechtomov, S. G., and Liebman, S. W. (1996) Genesis and variability of [PSI] prion factors in *Saccharomyces cerevisiae*. *Genetics* **144**, 1375–1386
 15. Schlumpberger, M., Prusiner, S. B., and Herskowitz, I. (2001) Induction of distinct [URE3] yeast prion strains. *Mol. Cell. Biol.* **21**, 7035–7046
 16. Bradley, M. E., Edskes, H. K., Hong, J. Y., Wickner, R. B., and Liebman, S. W. (2002) Interactions among prions and prion “strains” in yeast. *Proc. Natl. Acad. Sci. U.S.A.* **99**, 16392–16399
 17. Tanaka, M., Chien, P., Naber, N., Cooke, R., and Weissman, J. S. (2004) Conformational variations in an infectious protein determine prion strain differences. *Nature* **428**, 323–328
 18. Tanaka, M., Collins, S. R., Toyama, B. H., and Weissman, J. S. (2006) The physical basis of how prion conformations determine strain phenotypes. *Nature* **442**, 585–589
 19. Toyama, B. H., Kelly, M. J., Gross, J. D., and Weissman, J. S. (2007) The structural basis of yeast prion strain variants. *Nature* **449**, 233–237
 20. Derkatch, I. L., Bradley, M. E., Zhou, P., Chernoff, Y. O., and Liebman, S. W. (1997) Genetic and environmental factors affecting the *de novo* appearance of the [PSI⁺] prion in *Saccharomyces cerevisiae*. *Genetics* **147**, 507–519
 21. Derkatch, I. L., Bradley, M. E., Hong, J. Y., and Liebman, S. W. (2001) Prions affect the appearance of other prions. The story of [PIN⁺]. *Cell* **106**, 171–182
 22. Bradley, M. E., and Liebman, S. W. (2003) Destabilizing interactions among [PSI⁺] and [PIN⁺] yeast prion variants. *Genetics* **165**, 1675–1685
 23. Bagriantsev, S., and Liebman, S. W. (2004) Specificity of prion assembly *in vivo*. [PSI⁺] and [PIN⁺] form separate structures in yeast. *J. Biol. Chem.* **279**, 51042–51048
 24. Liebman, S. W., Bagriantsev, S. N., and Derkatch, I. L. (2006) Biochemical and genetic methods for characterization of [PIN⁺] prions in yeast. *Methods* **39**, 23–34
 25. Chien, P., and Weissman, J. S. (2001) Conformational diversity in a yeast prion dictates its seeding specificity. *Nature* **410**, 223–227
 26. Kushnirov, V. V., Kryndushkin, D. S., Boguta, M., Smirnov, V. N., and Ter-Avanesyan, M. D. (2000) Chaperones that cure yeast artificial [PSI⁺] and their prion-specific effects. *Curr. Biol.* **10**, 1443–1446
 27. Sondheimer, N., Lopez, N., Craig, E. A., and Lindquist, S. (2001) The role of Sis1 in the maintenance of the [RNQ⁺] prion. *EMBO J.* **20**, 2435–2442
 28. Morano, K. A., Grant, C. M., and Moye-Rowley, W. S. (2012) The response to heat shock and oxidative stress in *Saccharomyces cerevisiae*. *Genetics* **190**, 1157–1195
 29. Masison, D. C., Kirkland, P. A., and Sharma, D. (2009) Influence of Hsp70s and their regulators on yeast prion propagation. *Prion* **3**, 65–73
 30. Romanova, N. V., and Chernoff, Y. O. (2009) Hsp104 and prion propagation. *Protein Pept. Lett.* **16**, 598–605
 31. Summers, D. W., Douglas, P. M., and Cyr, D. M. (2009) Prion propagation by Hsp40 molecular chaperones. *Prion* **3**, 59–64
 32. Park, K.-W., Hahn, J.-S., Fan, Q., Thiele, D. J., and Li, L. (2006) *De novo* appearance and “strain” formation of yeast prion [PSI⁺] are regulated by the heat-shock transcription factor. *Genetics* **173**, 35–47
 33. Fan, Q., Park, K.-W., Du, Z., Morano, K. A., and Li, L. (2007) The role of Sse1 in the *de novo* formation and variant determination of the [PSI⁺] prion. *Genetics* **177**, 1583–1593
 34. Gietz, R. D., and Woods, R. A. (2002) Transformation of yeast by lithium acetate/single-stranded carrier DNA/polyethylene glycol method. *Methods Enzymol.* **350**, 87–96
 35. Herskowitz, I., and Jensen, R. E. (1991) Putting the HO gene to work. Practical uses for mating-type switching. *Methods Enzymol.* **194**, 132–146
 36. Rose, M. D., Winston, F. M., and Heiter, P. (1990) *Methods in Yeast Genetics: A Laboratory Course Manual*, Cold Spring Harbor Laboratory Press, Cold Spring Harbor, NY
 37. Scholz, O., Thiel, A., Hillen, W., and Niederweis, M. (2000) Quantitative analysis of gene expression with an improved green fluorescent protein. *Eur. J. Biochem.* **267**, 1565–1570
 38. Jansen, G., Wu, C., Schade, B., Thomas, D. Y., and Whiteway, M. (2005) Drag&Drop cloning in yeast. *Gene* **344**, 43–51
 39. Hanahan, D. (1983) Studies on transformation of *Escherichia coli* with plasmids. *J. Mol. Biol.* **166**, 557–580
 40. Kryndushkin, D. S., Alexandrov, I. M., Ter-Avanesyan, M. D., and Kushnirov, V. V. (2003) Yeast [PSI⁺] prion aggregates are formed by small Sup35 polymers fragmented by Hsp104. *J. Biol. Chem.* **278**, 49636–49643
 41. Feilotter, H. E., Hannon, G. J., Ruddell, C. J., and Beach, D. (1994) Construction of an improved host strain for two hybrid screening. *Nucleic Acids Res.* **22**, 1502–1503
 42. Chernoff, Y. O., Lindquist, S. L., Ono, B., Inge-Vechtomov, S. G., and Liebman, S. W. (1995) Role of the chaperone protein Hsp104 in propagation of the yeast prion-like factor [psi⁺]. *Science* **268**, 880–884
 43. Yu, H., Braun, P., Yildirim, M. A., Lemmens, I., Venkatesan, K., Sahalie, J., Hirozane-Kishikawa, T., Gebreab, F., Li, N., Simonis, N., Hao, T., Rual, J.-F., Dricot, A., Vazquez, A., Murray, R. R., Simon, C., Tardivo, L., Tam, S., Svrikapa, N., Fan, C., de Smet, A.-S., Motyl, A., Hudson, M. E., Park, J., Xin, X., Cusick, M. E., Moore, T., Boone, C., Snyder, M., Roth, F. P., Barabási, A.-L., Tavernier, J., Hill, D. E., and Vidal, M. (2008) High-quality binary protein interaction map of the yeast interactome network. *Science* **322**, 104–110
 44. Sindi, S. S., and Serio, T. R. (2009) Prion dynamics and the quest for the genetic determinant in protein-only inheritance. *Curr. Opin. Microbiol.* **12**, 623–630
 45. Derdowski, A., Sindi, S. S., Klaips, C. L., DiSalvo, S., and Serio, T. R. (2010) A size threshold limits prion transmission and establishes phenotypic diversity. *Science* **330**, 680–683
 46. Borchsenius, A. S., Müller, S., Newnam, G. P., Inge-Vechtomov, S. G., and Chernoff, Y. O. (2006) Prion variant maintained only at high levels of the Hsp104 disaggregase. *Curr. Genet.* **49**, 21–29
 47. Taipale, M., Jarosz, D. F., and Lindquist, S. (2010) HSP90 at the hub of protein homeostasis. Emerging mechanistic insights. *Nat. Rev. Mol. Cell Biol.* **11**, 515–528
 48. Borkovich, K. A., Farrelly, F. W., Finkelstein, D. B., Taulien, J., and Lindquist, S. (1989) hsp82 is an essential protein that is required in higher concentrations for growth of cells at higher temperatures. *Mol. Cell. Biol.* **9**, 3919–3930
 49. Prodromou, C., Siligardi, G., O’Brien, R., Woolfson, D. N., Regan, L., Panaretou, B., Ladbury, J. E., Piper, P. W., and Pearl, L. H. (1999) Regulation of Hsp90 ATPase activity by tetratricopeptide repeat (TPR)-domain co-chaperones. *EMBO J.* **18**, 754–762
 50. Panaretou, B., Siligardi, G., Meyer, P., Maloney, A., Sullivan, J. K., Singh, S., Millson, S. H., Clarke, P. A., Naaby-Hansen, S., Stein, R., Cramer, R., Mollapour, M., Workman, P., Piper, P. W., Pearl, L. H., and Prodromou, C. (2002) Activation of the ATPase activity of Hsp90 by the stress-regulated co-chaperone Aha1. *Mol. Cell* **10**, 1307–1318
 51. McLaughlin, S. H., Sobott, F., Yao, Z.-P., Zhang, W., Nielsen, P. R., Grossmann, J. G., Laue, E. D., Robinson, C. V., and Jackson, S. E. (2006) The co-chaperone p23 arrests the Hsp90 ATPase cycle to trap client proteins. *J. Mol. Biol.* **356**, 746–758
 52. Duina, A. A., Chang, H. C., Marsh, J. A., Lindquist, S., and Gaber, R. F. (1996) A cyclophilin function in Hsp90-dependent signal transduction. *Science* **274**, 1713–1715
 53. Mayr, C., Richter, K., Lilie, H., and Buchner, J. (2000) Cpr6 and Cpr7, two closely related Hsp90-associated immunophilins from *Saccharomyces cerevisiae*, differ in their functional properties. *J. Biol. Chem.* **275**, 34140–34146
 54. Kurahashi, H., Ishiwata, M., Shibata, S., and Nakamura, Y. (2008) A regulatory role of the Rnq1 nonprion domain for prion propagation and poly-

Chaperone-mediated Determination of [PIN⁺] Variants

- glutamine aggregates. *Mol. Cell. Biol.* **28**, 3313–3323
55. Wickner, R. B., Dyda, F., and Tycko, R. (2008) Amyloid of Rnq1p, the basis of the [PIN⁺] prion, has a parallel in-register β -sheet structure. *Proc. Natl. Acad. Sci. U.S.A.* **105**, 2403–2408
56. Abbas-Terki, T., Donzé, O., Briand, P. A., and Picard, D. (2001) Hsp104 interacts with Hsp90 cochaperones in respiring yeast. *Mol. Cell. Biol.* **21**, 7569–7575
57. Mackay, R. G., Helsen, C. W., Tkach, J. M., and Glover, J. R. (2008) The C-terminal extension of *Saccharomyces cerevisiae* Hsp104 plays a role in oligomer assembly. *Biochemistry* **47**, 1918–1927
58. Reidy, M., and Masison, D. C. (2010) Sti1 regulation of Hsp70 and Hsp90 is critical for curing of *Saccharomyces cerevisiae* [PSI⁺] prions by Hsp104. *Mol. Cell. Biol.* **30**, 3542–3552
59. Shaner, L., Sousa, R., and Morano, K. A. (2006) Characterization of Hsp70 binding and nucleotide exchange by the yeast Hsp110 chaperone Sse1. *Biochemistry* **45**, 15075–15084
60. Sharma, J., and Liebman, S. W. (2012) [PSI⁺] prion variant establishment in yeast. *Mol. Microbiol.* **4**, 866–881